Biochemical Pharmacology, Vol. 42, No. 11, pp. 2199–2208, 1991.
Printed in Great Britain.

0006-2952/91 $3.00 + 0.00

POLYPLOIDY INDUCTION AS A CONSEQUENCE OF TOPOISOMERASE INHIBITION

A FLOW CYTOMETRIC ASSESSMENT*

ROBERT M. ZUCKER,†‡ DAVID J. ADAMS,§ KENNETH W. BAIR‖ and KENNETH H. ELSTEIN†

†ManTech Environmental Technology, Inc., Research Triangle Park, NC 27709; and §Division of Cell Biology and ‖Division of Organic Chemistry, Wellcome Research Laboratories, Research Triangle Park, NC 27709, U.S.A.

(*Received* 3 *May* 1991; *accepted* 17 *July* 1991)

Abstract—Following recovery from a 4-hr exposure to clinically achievable concentrations of the topoisomerase II inhibitors Adriamycin®, teniposide, or amsacrine or the putative topoisomerase II inhibitor crisnatol, murine erythroleukemic cells remained viable for up to 48 hr, but did not proliferate. Cell cycle analysis after a 24-hr recovery revealed blocks in G_2 (4N DNA) or $>G_2$ (up to 8N DNA) polyploid stages. The relative percentages of cells in either stage was a function of drug concentration and cell cycle stage at time of exposure: typically, cells exposed during S phase became blocked in G_2, whereas those exposed during G_2/M progressed into $>G_2$ polyploid stages. G_2-blocked cells exhibited a 2- to 3-fold increase in nuclear protein content and cellular/nuclear volume (i.e. unbalanced growth) and ~5% more DNA stainability (as a consequence of nuclear conformational changes rather than redundant DNA synthesis). In all cases, at the drug concentrations studied, mitotic figures were absent and G_2 and $>G_2$ blocks were irreversible, indicating that the mechanism of polyploidy induction differs from that of microtubule inhibitors. These findings suggest that although topoisomerase inhibitors interfere with DNA synthesis in the S phase, their induction of $>G_2$ polyploid blocks may involve direct or indirect inhibition of chromosome condensation.

By transiently breaking DNA strands, the topos¶ play essential roles in DNA replication (e.g. unknotting supercoiled DNA) [1]. They are divided into two types depending on whether they introduce single-stranded (topo I) or double-stranded (topo II) breaks in their DNA substrates [2]. In addition to this S-phase role, there is evidence that topo II activity may contribute to chromosome condensation in early mitosis [3–6] and separation of entangled chromatids in late mitosis (anaphase) [7].

The observation that a number of efficacious chemotherapeutic agents inhibit topo I and/or topo II activity has generated considerable interest in understanding how topo inhibition contributes to the antitumor activity of these drugs [1]. Apparently, topo I [8] and topo II [1, 8] inhibitors act during DNA replication (S phase) by stabilizing the otherwise transient "cleavable complex" that forms between the enzyme and the nicked DNA. Although some topo II inhibitors also may inhibit chromosome condensation in mammalian cells [7, 9], the mechanism for this is not clear. Regardless, exposure of logarithmically growing cells to the topo inhibitors may cause any or all of the following: (i) inhibition of S-phase cell cycle traverse [10], (ii) inhibition of progression from the G_2 phase to the M phase of the cell cycle (i.e. G_2 block) [11, 12], (iii) unbalanced growth (i.e. continued synthesis of RNA and protein in the absence of DNA synthesis and cytokinesis) [13], and (iv) polyploidy [14].

To investigate factors influencing these manifestations of topo inhibitor activity, we used flow cytometry to analyze the cell cycle of Friend murine erythroleukemic cells (MELC) recovering from exposure to clinically achievable concentrations of the topo I inhibitor camptothecin (CPT); the topo II inhibitors Adriamycin® (ADR), amsacrine (*m*-AMSA), or teniposide (VM-26); or crisnatol (CRS), a DNA intercalator [15] and putative topoisomerase inhibitor [16]. MELC were used because they grow in suspension (thereby simplifying cellular and nuclear isolation) and can be synchronized easily, yet exhibit the same cell cycle response to these agents as the MDA-MB-231 line of human breast cancer cells (unpublished results).

Our approach was to study flow cytometric parameters of asynchronous and thymidine-synchronized MELC recovering from exposure to topo

* The research described in this article has been funded wholly or in part by the Health Effects Research Laboratory, U.S. Environmental Protection Agency under Contract 6802-4450 to ManTech Environmental Technology, Inc. It has been reviewed and approved for publication as an EPA document. Approval does not signify that the contents necessarily reflect the views and policies of the Agency nor does mention of trade names or commercial products constitute endorsement or recommendation for use.

‡ Corresponding author.

¶ Abbreviations: ADR, Adriamycin®; *m*-AMSA, amsacrine; AMT, metantrone; BrdU, 5-bromodeoxyuridine; BSA, bovine serum albumin; CF, 5,6-carboxyfluorescein; CFDA, 5,6-carboxyfluorescein diacetate; CHO, Chinese hamster ovary cells; CPT, camptothecin; CRS, crisnatol; DMSO, dimethyl sulfoxide; FITC, fluorescein isothiocyanate; MELC, Friend murine erythroleukemic cells; PBS, phosphate-buffered saline; PI, propidium iodide; topo, topoisomerase; VM-26, teniposide; and VP-16, etoposide.

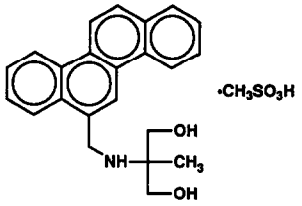

Fig. 1. Chemical structure of the new DNA intercalator and putative topo II inhibitor crisnatol (CRS), a chrysene derivative containing a methylaminopropanediol side chain [15, 16].

inhibitors. In addition to membrane integrity (viability), we investigated nuclear fluorescein isothiocyanate (FITC) fluorescence and/or 90° light scatter (protein content [17]), ability to incorporate 5-bromodeoxyuridine (BrdU), and perturbations in the DNA distribution [18]. We also used Coulter electronic analysis to measure drug effects on growth (i.e. increase in cell number) and on cellular and nuclear volume [19].

Our results indicate that following a 4-hr exposure to relatively low concentrations of topo inhibitors or CRS, recovering MELC became blocked in either the tetraploid G_2 phase or in a continuum of >4N polyploid stages, with G_2-blocked cells exhibiting unbalanced growth [13] and ~5% more DNA stainability than control G_2 cells. The relative proportion of cells in each of these stages was a function of both drug concentration and cell cycle stage at time of exposure. By 72 hr post-exposure, there was no sign of growth and viability decreased, suggesting that the drug-induced blocks were terminal. Moreover, the absence of mitotic figures (as determined microscopically) suggests a different mechanism of polyploidy induction than that of microtubule inhibitors [20].

MATERIALS AND METHODS

Cell culture. MELC (T3CL2, obtained from Dr. Clyde Hutchison, University of North Carolina, Chapel Hill, NC) were maintained in logarithmic growth in RPMI 1640 (No. 320-1875, GIBCO, Grand Island, NY) supplemented with 10% fetal bovine serum (GIBCO No. 203-6140) and 25 mM HEPES (No. H3375, Sigma Chemical Co., St. Louis, MO) at 37° in an atmosphere of 5% CO_2 in air.

Exposure protocol. MELC were exposed to 0.5 μg/mL (1.4 μM) CPT, 1.0 μg/mL (1.5 μM) VM-26, 0.5 μg/mL (0.9 μM) ADR, 1.0 μg/mL (2.5 μM) *m*-AMSA, or 4.4 μg/mL (10 μM) CRS for 4 hr, washed of drug, and recultured in drug-free medium prior to analysis. Drug concentrations were established from preliminary studies. CRS (Fig. 1) was obtained from Burroughs Wellcome Laboratories (Research Triangle Park, NC); CPT (No. 94600), *m*-AMSA (No. 249992), and VM-26 (No. 122819) were obtained from the National Cancer Institute Drug Development Branch, Bethesda, MD; ADR (No. D1515) was obtained from Sigma. All drugs were dissolved in dimethyl sulfoxide (DMSO) (Sigma No. D5879). The final concentration (0.1%) of DMSO used in the culture medium had no detectable effect on growth, viability, or any other flow cytometric parameter.

Flow cytometry. Flow cytometric analyses were made with an Ortho 50H cytofluorograph (Becton-Dickinson, Westwood, MA) equipped with an analytical flow cell (30H) and a 100 mW, 488 nm-line argon-ion laser (model 75, Lexel, Inc., Fremont, CA). Flow rate was maintained at 200 particles/sec while analyzing 10^4 cells or nuclei per sample. For two-color (green/red) fluorescence analyses, compensation circuitry was used to offset any signal cross-detection. In addition to fluorescence excitation, the argon-ion laser was used to generate nuclear 90° light scatter (protein [17]). Data were collected, stored, and manipulated via an Ortho 2150 computer system.

Viability assay. Viability was assessed by the 5,6-carboxyfluorescein diacetate/propidium iodide (CFDA/PI) assay [18]. CFDA (No. C-195, Molecular Probes, Eugene, OR) was added to approximately 2×10^5 MELC in 1 mL growth medium to a final concentration of 3.6 μg/mL from a stock solution of 2 mg/mL in acetone diluted 1:50 with phosphate-buffered saline (PBS) (GIBCO No. 310-4080). The final acetone concentration (0.2%, v/v) had no effect on cellular viability or 5,6-carboxyfluorescein (CF) retention. The cells were incubated for 10 min at 37° and chilled on ice. PI (Sigma No. P4170) was added from a stock solution of 50 μg/mL PBS to a final concentration of 4.5 μg/mL and the cells were analyzed at 0°. Viability was estimated as the percentage of cells exhibiting green (CF) fluorescence (derived from the esterase-catalyzed hydrolysis of nonfluorescent CFDA), but not red (PI) fluorescence (resulting from DNA intercalation).

Sorting. To verify that G_2 (4N) doublets could be discerned electronically from single 8N nuclei (and therefore eliminated from registering in the same histogram channels), we sorted the nuclei of MELC exposed for 24 hr to 1.1 μg/mL CRS. Nuclei were sorted (500/sec, using the Ortho/BD 75 μM orifice sorting cell [50H] and 0.85% saline as the sorting medium), collected on ice, and subsequently reanalyzed.

Growth and cellular volume measurements. The effects of the topo inhibitors on growth (increase in cell number over seed) and on cellular and nuclear volume were measured with a Coulter Counter (model ZBI) and Channelyzer (model 20; Coulter Electronics, Hialeah, FL). Nuclei were obtained from PBS-washed cells lysed by a 20-min incubation (19°) in 0.2% Nonidet P-40 (Sigma No. N6507) in PBS. Prior to volumetric analysis, isolated nuclei and cells sampled directly from culture were fixed in 3% aqueous glutaraldehyde (EM Science No. GX015305-1, Cherry Hill, NJ) [19].

Nuclear protein and cell cycle analysis. Nuclei were isolated from PBS-washed MELC (0.5 to 1.0×10^6 cells per sample) by a 30-min incubation (19°) in 0.2% Nonidet P-40 supplemented with 0.5 mg/mL RNase A (Sigma No. R4875). The lysates were chilled on ice and stained with 50 μg/mL PI for DNA

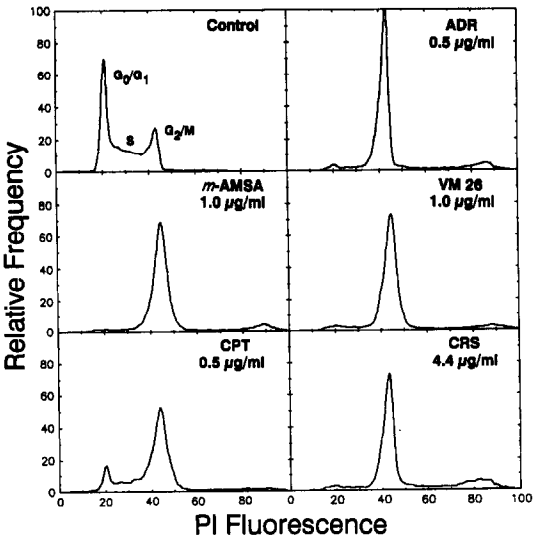

Fig. 2. DNA distributions of MELC 24 hr after a 4-hr pulse exposure to topo I or topo II inhibitors.

content and 1.5 μg/mL FITC (Sigma No. F7250) for protein content.

The relative percentage of nuclei in the G_0/G_1, S, and G_2/M phases of the cell cycle were estimated using *Multicycle* (Phoenix Flow Systems, San Diego, CA), a PC-based software package employing the mathematical model of Dean and Jett [21]. Those nuclei located in the region beyond the Gaussian distribution of G_2 (as estimated by *Multicycle*) were considered to be >4N polyploid (>G_2). As such, estimation of polyploid cell percentage was not influenced by shifts in the location of the G_2 peak along the PI fluorescence scale.

Synchronization. To assess the effect of cell cycle stage at time of exposure on the resulting DNA distributions, MELC (doubling time ~12 hr) were synchronized using a double-thymidine block [19]. Briefly, 1×10^5 MELC/mL RPMI were exposed to 0.5 mg/mL thymidine (Sigma No. T5018) for 8 hr (to block late S and G_2/M cells at the G_1/S interface), washed and recultured for 5.5 hr (to accumulate cells between S and G_2/M phases), and blocked a second time with 0.5 mg/mL thymidine for 8–9 hr prior to washout. At 2-hr intervals following washout, MELC were exposed to either VM-26 (0.25 to 1.0 μg/mL) or ADR (0.05 or 0.5 μg/mL) for 2 hr, washed, and recultured overnight. By so doing, the majority of cells were in either the G_1/S (T = 0 hr), S (T = 2 hr), G_2/M (T = 4 hr) or M and G_0/G_1 (T = 6 hr) phase(s) at the time of exposure.

DNA synthesis. The ability of >G_2 cells to synthesize DNA was assessed by the BrdU incorporation assay [22]. Approximately 1×10^6 cells per sample were exposed to the thymidine analog BrdU for the last 30 min of recovery from exposure to CRS (4.4 μg/mL), ADR (0.5 μg/mL), or VM-26 (1.0 μg/mL). Washed cells were fixed in 70% ethanol overnight at 5° and then denatured with 4 N HCl, washed in 0.5% bovine serum albumin (BSA) (Fraction V, No. 2293-01, Armour Pharmaceutical Co., Kankakee, IL) in PBS containing 0.5% Tween 20 (Sigma No. P1379), and incubated (30 min, 19°) with anti-BrdU (Becton-Dickinson No. 7580). Samples were washed in PBS/BSA/Tween and incubated (30 min, 19°) with FITC-conjugated goat anti-mouse IgG (No. 605-29, Boehringer-Mannheim Biochemicals, Indianapolis, IN) prior to chilling on ice and staining with PI (50 μg/mL). Only cells incorporating BrdU during DNA synthesis exhibit FITC fluorescence.

Höechst staining. To ensure that the ~5% increase in PI fluorescence exhibited by G_2-blocked cells was not due to artifacts inherent in the PI-FITC staining procedure (i.e. incomplete RNase digestion, fluorochrome binding differences, or incomplete double fluorescence compensation), MELC exposed to *m*-AMSA (0.1 μg/mL, 4 hr with agent/18 hr without) were lysed in the presence or absence of RNase and stained with 5 μg/mL Höechst 33342 (Sigma No. B2261), which specifically stains DNA by binding to the minor groove (in contrast to PI, which intercalates both RNA and DNA) [23]. Also, to ensure that the increased PI fluorescence was not an artifact of staining variability, control and *m*-AMSA-exposed cells were mixed prior to cytolysis and staining so that G_0/G_1 peaks could be aligned.

Cytology. Cytological samples were prepared by

Table 1. MELC cellular and nuclear parameters 24 hr post-exposure

Concentration (μg/mL)	% PI excl.	Growth	Cell. vol.	Nucl. vol.	90° Scat.	%G_2	%>G_2
Control	99	4.8	1.0	1.0	1.0	12.0	2.8
ADR (0.5)	98	1.0	2.0	2.0	2.1	48.5	12.8
m-AMSA (1.0)	97	1.0	2.8	2.2	2.5	63.1	19.6
VM-26 (1.0)	95	1.0	2.9	2.3	2.6	77.7	15.5
CPT (0.5)	98	1.1	3.0	2.2	2.3	53.7	13.3
CRS (4.4)	97	0.9	2.2	2.0	2.2	65.3	22.8

The effects of topo inhibitors on percent PI exclusion (viability), growth (expressed as fold increase over seed), Coulter cellular and nuclear (electronic) volumes, the 90° light scatter (protein content [17]) of G_2 nuclei, and the relative percentages of G_2 and >G_2 nuclei were determined. The parameters were measured 24 hr after a 4-hr pulse exposure, as described in Materials and Methods.

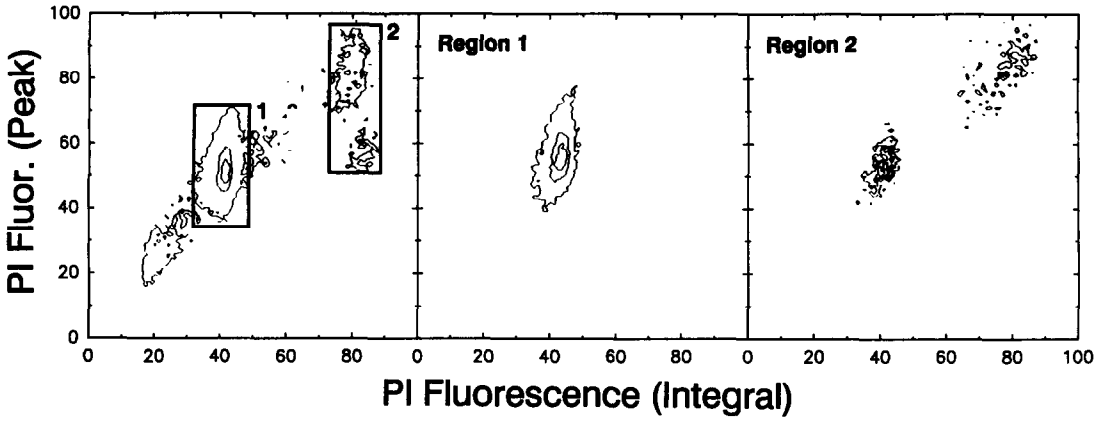

Fig. 3. Bivariate distributions of the peak versus the integral of the PI fluorescence signal of nuclei isolated from MELC exposed to 1.1 μg/mL CRS for 24 hr. The nuclei in Regions 1 and 2 were sorted and reanalyzed to validate electronic doublet discrimination of nucleic exhibiting increased PI fluorescence.

a cytocentrifugation technique [24] for examination of changes in morphology and mitotic index.

Data. The reported data are representative of a series of replicated experiments that were all internally consistent.

RESULTS

MELC recovering (24 hr) from a 4-hr exposure to the topo I inhibitor CPT, the topo II inhibitors ADR, *m*-AMSA, or VM-26, or the putative topo II inhibitor CRS accumulated in both the tetraploid G_2 phase of the cell cycle and a continuum of >4N–8N polyploid stages (Fig. 2). The nuclei of G_2-blocked MELC exhibited a 2- to 3-fold increase in mean 90° light scatter (protein content [17]) coincident with a 2- to 3-fold increase in mean cellular and nuclear volumes (Table 1), suggestive of unbalanced growth. Although cells exposed to topo II inhibitors remained viable (i.e. excluded PI) 24 hr into recovery, viability decreased to 75–85% by 48 hr and to 50–75% by 72 hr. Moreover, there was no growth (increase in cell number) during the 72-hr period, suggesting that these blocks were terminal. However, there was a small subpopulation among CPT-exposed cells that was either unaffected by drug exposure or capable of repairing the damage and then proliferating (Fig. 2).

To verify that the observed $>G_2$ polyploidy was not an artifact resulting from adherent nuclei (physical doublets) or successive nuclei registering erroneously as one particle (temporal doublets), we sorted the subpopulations appearing on a bivariate distribution of the peak versus the integral of the PI fluorescence signal (Fig. 3). Such "peak vs area" analysis is used routinely to discriminate G_0/G_1 doublets from G_2/M nuclei. Typically, the peak of the PI fluorescence signal of G_0/G_1 doublets is lower than that of a single G_2/M nucleus, although the integrals of the fluorescence signals are identical. To prove the validity of electronic discrimination at elevated PI fluorescence levels, the G_2 and $>G_2$ nuclei of MELC exposed to 1.1 μg/mL CRS for 24 hr were sorted and reanalyzed. CRS was used because in preliminary tests it induced cell cycle perturbations similar to those caused by the other agents but with a larger percentage of >4N cells (Table 1). Although microscopic inspection of the sorted samples revealed no doublets (presumably because of post-sorting separation of physical doublets), reanalysis revealed that the cluster exhibiting low peak fluorescence was composed of doublets (either physical or temporal), while the cluster exhibiting high peak fluorescence was composed of single nuclei. Moreover, we observed that ≥85% of recovering topo II-inhibitor-exposed cells containing between 4N and 8N DNA incorporated BrdU*, which substantiates that the increased PI fluorescence is the result of continued DNA synthesis.

To get an approximation of the time frame of MELC progression into G_2 and $>G_2$ phases, we used nuclear peak versus area analysis to monitor (over 48 hr) recovery from a 4-hr exposure to topo inhibitors (Figs. 4 and 5). Progression into G_2 and beyond was most rapid within the first 12 hr. Thereafter, progression beyond G_2 continued at a slower rate and then stopped after 48 hr, concurrent with a decrease in viability.

To gain a better understanding of factors influencing cell progression into abnormal polyploid stages, we exposed (2 hr) both asynchronous and thymidine-synchronized MELC to VM-26 or ADR at 2-hr intervals following release from synchronization, washed the cells, and recultured them overnight. Following exposure to VM-26, more than 40% of MELC synchronized in G_2/M (T = 4 hr) exhibited $>G_2$ polyploidy (Fig. 6). In contrast, the phase-specificity of ADR in producing $>G_2$ cells was a function of concentration (Fig. 7, Table 2). At

* Exact percentages incorporating BrdU; 85% following exposure to 0.5 μg/mL ADR, 88% following 4.4 μg/mL CRS, and 89% following 1.0 μg/mL VM-26.

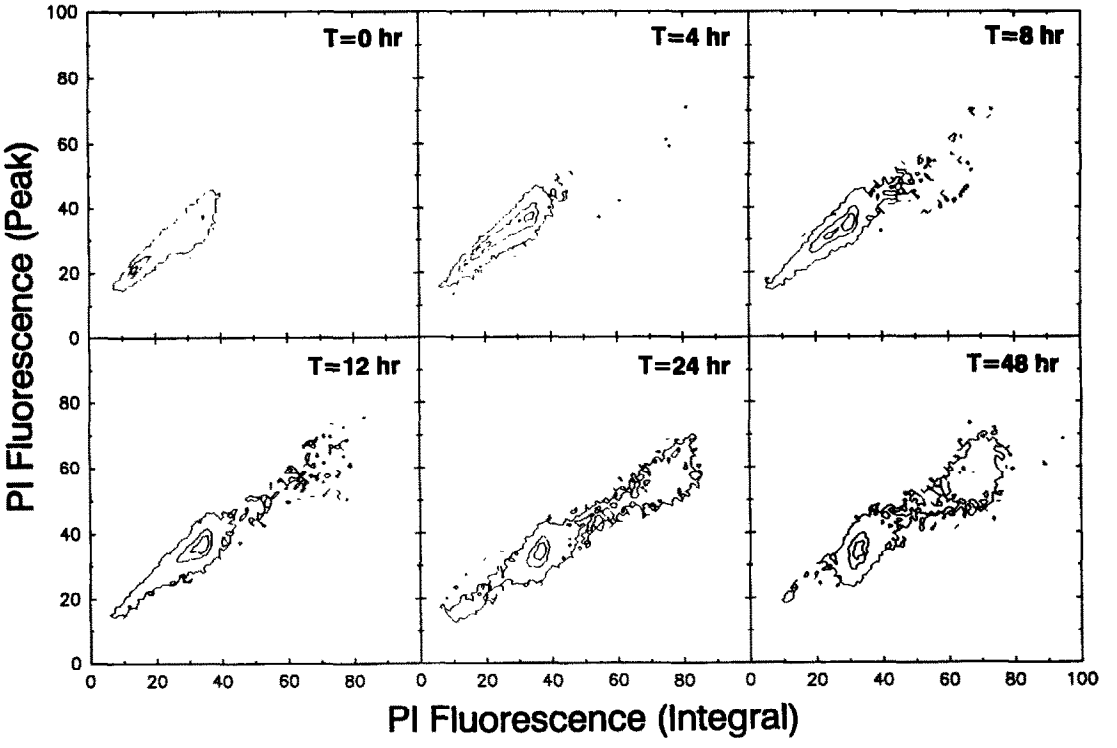

Fig. 4. Time-dependent progression into G_2 and $>G_2$ phases. Doublet discriminated bivariate distributions of PI fluorescence peak versus integral signals were used to monitor the recovery (over 48 hr) of MELC exposed to 4.4 μg/mL CRS for 4 hr. Similar results from exposure to the other chemotherapeutic agents are summarized in Fig. 5.

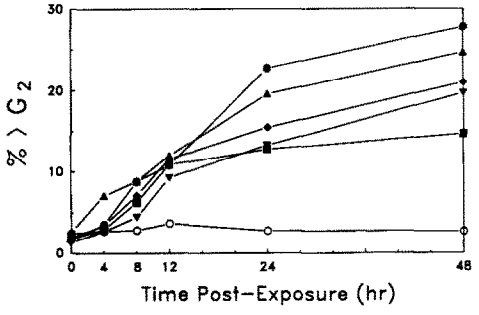

Fig. 5. Time-dependent accumulation of $>G_2$ nuclei. The percentages of $>G_2$ nuclei were measured over a 48-hr recovery from a 4-hr exposure to topo inhibitors. Data were derived from distributions like those displayed in Fig. 4. Key: (○) control; (■) 0.5 μg/mL (0.9 μM) ADR; (▼) 0.5 μg/mL (1.4 μM) CPT; (◆) 1.0 μg/mL (1.5 μM) VM-26; (▲) 1.0 μg/mL (2.5 μM) *m*-AMSA; and (●) 4.4 μg/mL (10 μM) CRS.

0.5 μg/mL, ADR exposure revealed G_2/M-phase (T = 4 hr) specificity similar to that of VM-26; however, at 0.05 μg/mL, substantial 8N-cell induction occurred in MELC traversing S phase (T = 0, 2 hr) at time of exposure.

We also observed that, in addition to the 2- to 3-fold increase in FITC (protein) fluorescence, the nuclei of MELC blocked in G_2 by exposure to topo inhibitors exhibited an ~5% increase in PI (DNA) fluorescence (Fig. 8). Since the PI staining protocol involves pretreatment with RNase and simultaneous staining with FITC, we verified that the increased PI fluorescence was not an artifact of undigested RNA, fluorochrome binding, or incomplete double fluorescence compensation by staining lysed *m*-AMSA-exposed cells with Höechst 33342, which specifically stains DNA [23]. Also, to control for the possibility that RNA predigestion could alter nucleosome conformation and, consequently, increase fluorochrome binding, we lysed paired samples in both the absence and presence of RNase. Our observation of a 3% (without RNase) to 5% (with RNase) increase in Höechst fluorescence suggests that the ~5% increase in PI fluorescence was not attributable to staining or electronic artifacts (data not shown).

DISCUSSION

Exposure of MELC for 4 hr to topo I or topo II inhibitors or CRS followed by recovery in drug-free medium resulted in accumulation of cells in either the G_2 phase or a continuum of >4N–8N stages (Fig. 2, Table 1), but few (<1%) or no mitotic figures (control = 5%).

G_2 block. After observing G_2 blocks in Chinese hamster ovary cells (CHO) exposed to a number of

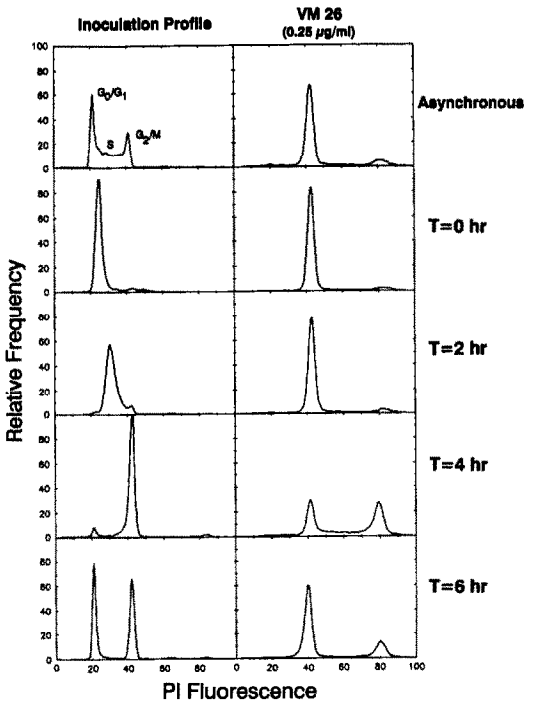

Fig. 6. DNA histograms of the nuclei of synchronous and asynchronous MELC exposed to 0.25 μg/mL VM-26 for 2 hr followed by washout and reculture. (Similar data from 0.5 and 1.0 μg/mL exposures are not shown.) Cells were exposed for 0 (G_1/S), 2 (S), 4 (G_2/M) or 6 (M, G_0/G_1) hr after release from thymidine-induced synchronization.

chemotherapeutic agents, Tobey [11] hypothesized the G_2 phase as a surveillance mechanism to eliminate from proliferation mode those cells with altered DNA. The mechanism preventing G_2-cell progression into the M phase also has been attributed to an inability of cells to transcribe damaged DNA into the mRNA necessary for progression into mitosis [25], to inability to synthesize essential proteins [12], and to inhibition of $p34^{cdc2}$ kinase, a cell-regulated protein necessary for nuclear envelope disassembly, chromosome condensation, and construction of the mitotic spindle [26].

Concurrent with G_2 blocks, others have noted cell enlargement as a result of "unbalanced growth" (i.e. continued RNA and protein synthesis in the absence of DNA synthesis or cytokinesis [13, 27, 28]). Our observation of increased cellular/nuclear volume and nuclear protein content in cells terminally blocked in G_2 (Table 1, Fig. 8) is consistent with the induction of unbalanced growth as a consequence of an inability to progress into mitosis. However, we also observed a 5% increase in DNA stainability (Fig. 8) with both the DNA intercalator PI and the DNA outside binder Höechst 33342 [23].

Upon observing similar increases in CHO and mouse lymphoma cells exposed to hydroxyurea, Hill and Schimke [29] hypothesized increased DNA content as a result of gene amplification. However, given that our MELC contain approximately 60 chromosomes, a 5% increase in G_2/M DNA content would require replication of the equivalent of 2–3 entire chromosomes, which seems unlikely. Conversely, it seems doubtful that over-replication of a few genes would result in a fluorescence increase of 5%. Although we detected increased stainability with two fluorochromes, the conclusion that this signifies increased DNA synthesis may be premature.

Darzynkiewicz [30] noted that chromatin condensation during spermiogenesis or DMSO-induced differentiation of MELC decreases DNA accessibility to fluorochrome binding. As such, one would expect that decondensed chromatin would be more accessible to fluorochromes, as is supported by our observation of increased Höechst fluorescence in RNase-treated samples. Indeed, Evenson *et al.* [31] proposed a similar explanation for increased acridine orange stainability of MELC exposed to metantrone (AMT). Clearly, studies using other methodologies are in order, but until this matter is resolved, investigators detecting "aneuploidy" near the G_0/G_1 or G_2/M peaks in cells exhibiting biophysical changes suggestive of chromatin decondensation (e.g. increased nuclear volume/protein content, no mitotic figures) should exercise caution in their interpretation.

$>G_2$ polyploidy. In addition to G_2 blockage, concentration-dependent increases in the percentages of $>G_2$ cells have been noted in several different cell lines exposed to a variety of compounds including alkylating agents [32] and topo II [14], microtubule [33], and metabolic [32] inhibitors. Schimke and coworkers [34] explained hydroxyurea- and aphidicholin-induced >4N polyploidy as one of several manifestations of DNA over-replication. Following drug removal, these polyploid cells continued cycling and could enter M phase at variable times during the second S-phase cycle.

The 2-fold increase in DNA stainability exhibited by MELC exposed to topo inhibitors or CRS is too great to be the result of conformational changes given the binding efficiency of PI [30]. Rather, it is probably a function of redundant DNA synthesis, as is supported by our observation that ≥85% of cells containing between 4N and 8N DNA incorporated BrdU. Moreover, we observed induction of the maximal percentage of >4N MELC by VM-26 (Fig. 6), 0.5 μg/mL ADR (Fig. 7), and CPT [35] in cells traversing G_2/M at the time of exposure. However, MELC exposed to topo II inhibitors did not exhibit mitotic figures or evidence of cycling (i.e. reappearance of G_0/G_1- or S-phase nuclei) even 72 hr after drug removal. Instead, viability decreased. This suggests a different mechanism than either that resulting from the DNA synthesis inhibitors hydroxyurea and aphidicolin (which presumably involves DNA over-replication [34]), or that resulting from microtubule inhibitors (e.g. vinblastine or taxol), which induce M-phase blocks [20]. Rather, it suggests that topo inhibitors can act specifically in the G_2/M stage.

Action of topoisomerase inhibitors in G_2/M. Chow and Ross [36] correlated increased etoposide (VP-16)-induced DNA cleavage in G_2/M-phase cells with marked increases in topoisomerase II content, in contrast to the increased cytotoxicity resulting from S-phase exposure. Estey *et al.* [37] obtained similar

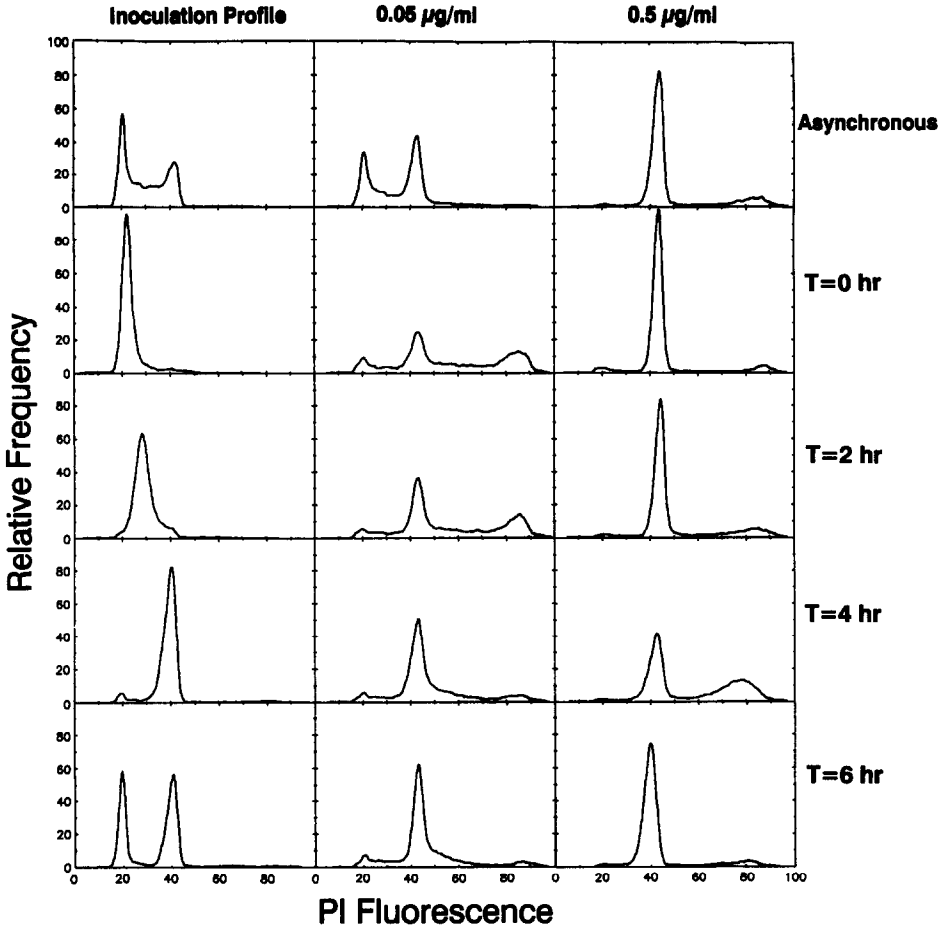

Fig. 7. DNA histograms of the nuclei of synchronous and asynchronous MELC exposed to 0.05 or 0.5 μg/mL ADR for 2 hr followed by washout and reculture.

Table 2. Effects of ADR exposure on synchronous and asynchronous MELC

Concentration (μg/mL)	Viability (% PI excl.)	Cell cycle analysis			
		$\%G_0/G_1$	%S	$\%G_2$	$\%>G_2$
Asynch. control	96	23.9	63.3	11.2	1.7
(0.05)	97	15.8	38.6	38.0	7.6
(0.5)	97	0.3	11.3	72.9	15.5
T = 0 (G_1/S)	97	0.0	96.0	2.3	1.7
(0.05)	97	5.2	8.9	36.0	50.0
(0.5)	95	2.2	6.0	82.6	9.3
T = 2 (S)	98	0.7	96.9	0.2	2.3
(0.05)	96	2.2	10.3	45.1	42.4
(0.5)	96	14.8	3.2	62.9	19.1
T = 4 (G_2/M)	98	0.8	29.3	66.9	2.9
(0.05)	95	2.7	10.3	65.0	22.0
(0.5)	95	1.8	0.0	53.9	44.3
T = 6 (M, G_0/G_1)	98	33.7	18.4	44.6	3.3
(0.05)	94	3.6	13.3	66.1	17.1
(0.5)	96	3.2	6.7	80.5	9.7

MELC were exposed to ADR for 2 hr at various intervals following release from synchronization and then washed and recultured. Cell cycle data were derived from histograms depicted in Fig. 7 with the G_1/S peak at T = 0 taken as early S phase. Control values represent DNA distributions at the time of ADR exposure; following recovery, all controls exhibited normal asynchronous distributions with $\leq 2\%$ in $>G_2$ phases.

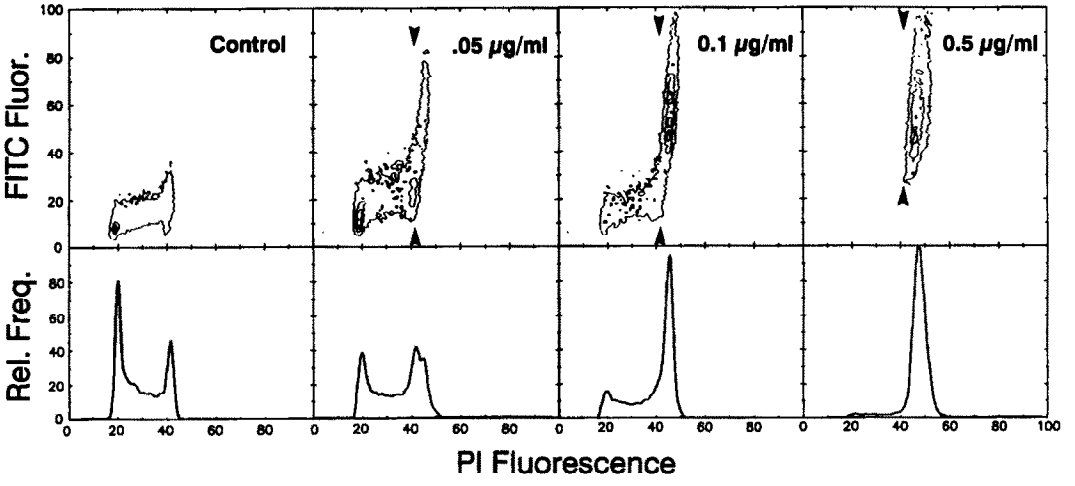

Fig. 8. Bivariate distributions (FITC vs PI fluorescence) and accompanying DNA histograms of the nuclei of MELC recovering (19 hr) from a 6-hr exposure to 0.05 to 0.5 μg/mL *m*-AMSA. Arrowheads denote the PI fluorescence of control G_2 nuclei.

results with *m*-AMSA. As such, the inhibition of chromosome condensation in MELC exposed to topo inhibitors during G_2/M traverse may be an indirect result of increased DNA damage. However, it seems unlikely that these severely damaged cells then would be able to continue a second round of DNA synthesis.

Indeed, given the concentration-dependence of topo inhibitor-induced strand scission [38], our observation that exposure to high drug concentrations during early to middle S-phase traverse (T = 0, 2 hr) resulted in few $>G_2$ cells (Figs. 6 and 7) suggests that extensive DNA damage may inhibit redundant DNA synthesis. That is, although unrepaired or incorrectly repaired DNA damage prevents proper chromosome packaging, it does not induce $>G_2$ polyploidy. Instead, affected cells become blocked in a state characterized by redundant RNA and protein synthesis (i.e. unbalanced growth) as well as increased stainability of the uncondensed chromatin (Figs. 6 and 7). Accordingly, the induction of redundant DNA synthesis (and, perhaps, inhibition of chromosome condensation) is likely due to another mechanism related to the action of topoisomerase inhibitors in G_2/M.

Studies with fission yeast, chicken lymphoblasts, and HeLa cells suggest that increased topo II activity in G_2/M correlates with a number of normal chromosome functions including condensation and separation at anaphase [3, 4, 39]. Thus, by interfering with topo function in G_2/M, inhibitors may directly prevent subsequent chromosome condensation.

However, it also is possible that the action of topoisomerase inhibitors is indirect. VP-16 markedly reduces the activity of $p34^{cdc2}$ kinase [26] which, in addition to its M-phase roles, may phosphorylate, and thereby initiate the removal of, several DNA-bound nuclear proteins to allow maximal DNA condensation [40]. Moreover, in BHK cells VM-26 blocks histone H1 and H3 phosphorylation and not only prevents chromosome condensation but decondenses previously condensed chromosomes [9]. Since topo II itself may need to be phosphorylated to be active in mitosis [39], these agents may inhibit chromosome condensation indirectly by inhibiting normal phosphorylation processes that prevent either topo II activation or the removal of physically hindering DNA-bound proteins.

How cells incapable of undergoing mitosis can then continue to synthesize DNA is not clear. In eukaryotic cells, the cyclical synthesis and degradation of cyclin, which binds to $p34^{cdc2}$ kinase (or a homologue) to form M-phase promoting factor (MPF), are responsible for the cyclical induction and termination of mitosis [41]. As such, not only might a perturbation of MPF synthesis or activation inhibit mitotic induction, but it is conceivable that cells incapable of condensing chromatin but capable of degrading cyclin would resume DNA synthesis once depressed cyclin levels rise and initiate another cell cycle. If true, this would suggest that $p34^{cdc2}$ kinase is a common factor in both drug-mediated inhibition of chromosome condensation and induction of $>G_2$ polyploidy.

It is of interest to note that the topo I inhibitor CPT induced cell cycle perturbations similar to those of the topo II inhibitors. However, a small percentage of CPT-exposed cells continued to cycle (Fig. 2) and of those affected, fewer exhibited $>G_2$ polyploidy (e.g. only ~25% of CPT-exposed G_2/M-synchronized MELC exhibited >4N DNA compared to ~50% for VM-26 [35] and >50% for ADR [Table 2] and CRS [data not shown]). A similar attenuation of effect was noted by Roberge *et al.* [9] who observed that VM-26 inhibited chromosome condensation if added during any stage of G_2, but CPT was effective only when applied during early G_2. Although the reason for this is unclear, it suggests that chromosomal inhibition and polyploidy induction are not specific to topo II inhibitors.

In addition to the discrepancies between topo I and topo II inhibitors, we observed that ADR, in contrast to VM-26, exhibited an underlying concentration-dependency in its phase-specificity of polyploidy induction (Fig. 7, Table 2). However, this is not inconsistent with the hypothesis of a G_2/M role for topo II. Unlike the epipodophyllotoxin derivatives VM-26 and VP-16, which do not bind to DNA, ADR intercalates DNA and persists at reduced concentrations following washout [42]. Moreover, ADR-induced strand breaks are more persistent [43, 44] and, consequently, as much as 30-fold more toxic than those induced by other topo II inhibitors [38]. It is possible, therefore, that at low concentrations, the combination of moderate S-phase damage and the presence of the intercalated agent may prevent chromosome condensation during G_2, yet allow redundant DNA synthesis. Yet at high concentrations, S-phase damage may be so severe that the majority of cells cannot progress to the G_2/M phase transition point preceding induction of a second round of DNA synthesis (i.e. >4N polyploidy). In contrast, exposure during G_2/M traverse results in a concentration-dependent increase in the percentage of $>G_2$ polyploid cells, possibly reflecting concentration-dependent damage to chromatin condensation mechanisms.

In summary, our investigation of the effects of topo inhibitors and CRS on MELC revealed that following removal of the drug, exposed cells became blocked in either G_2 or a continuum of >4N–8N polyploid stages (depending on concentration and cell cycle stage at time of exposure). Moreover, there was no evidence of reversibility or of mitotic figures as a consequence of direct (via topo II inhibition) or indirect (via inhibition of phosphorylation or extensive DNA damage) inhibition of chromosome condensation. Cells blocked in G_2 exhibited unbalanced growth (as a consequence of inhibition of karyo- and cytokinesis) and increased DNA stainability (most probably as a consequence of conformational changes resulting in enhanced accessibility of the DNA to fluorochrome binding). The higher polyploidy resulted predominantly from drug exposure during G_2/M and may be due to the uncoupling of chromosome condensation processes from mitotic regulation. Given the association of tetraploidy (and subsequent chromosome loss) with neoplastic transformation [45], it is conceivable that such an uncoupling may play a role in carcinogenesis.

Acknowledgements—We thank Dr. Robert Kavlock and Dr. John Rogers of the Developmental Toxicology Division of HERL/EPA and Dr. Richard Scearce of ManTech Environmental Technology, Inc. for their support throughout the course of this study, Dr. Edward Massaro of DTD/HERL/EPA for his helpful comments, and Dr. Karl Flora of the National Cancer Institute Drug Development Branch for providing the cited chemotherapeutic agents.

REFERENCES

1. D'Arpa R and Liu LF, Topoisomerase-targeting antitumor drugs. *Biochim Biophys Acta* **989**: 163–177, 1989.
2. Liu LF, DNA topoisomerases—Enzymes that catalyze the breaking and rejoining of DNA. *CRC Crit Rev Biochem* **15**: 1–24, 1983.
3. Gasser SM, Laroche T, Falquet J, Boy de la Tour E and Laemmli UK, Metaphase chromosome structure: Involvement of topoisomerase II. *J Mol Biol* **188**: 613–629, 1986.
4. Uemura T, Ohkura H, Adachi Y, Morino K, Shiozaki K and Yanagida M, DNA topoisomerase II is required for condensation and separation of mitotic chromosomes in *S. pombe*. *Cell* **50**: 917–925, 1987.
5. Holm C, Goto T, Wang JC and Botstein D, DNA topoisomerase II is required at the time of mitosis in yeast. *Cell* **41**: 553–563, 1985.
6. Rowley R and Kort L, Novobiocin, nalidixic acid, etoposide, and 4′-(9-acridinylamino)methanesulfon-*m*-anisidide effects on G_2 and mitotic Chinese hamster ovary cell progression. *Cancer Res* **49**: 4752–4757, 1989.
7. Holm C, Stearns T and Botstein D, DNA topoisomerase II must act at mitosis to prevent chromosome nondisjunction and chromosome breakage. *Mol Cell Biol* **9**: 159–168, 1989.
8. Hong JH, DNA topoisomerase: The mechanism of resistance to DNA topoisomerase II inhibitor VP-16. *Hiroshima J Med Sci* **38**: 197–207, 1989.
9. Roberge M, Th'ng J, Hamaguchi J and Bradbury EM, The topoisomerase II inhibitor VM-26 induces marked changes in histone H1 kinase activity, histones H1 and H3 phosphorylation, and chromosome condensation in G2 phase and mitotic BHK cells. *J Cell Biol* **111**: 1753–1762, 1990.
10. Krishan A, Paika K and Frei E III, Cytofluorometric studies on the action of podophyllotoxin and epipodophyllotoxins (VM-26, VP-16-123) on the cell cycle traverse of human lymphoblasts. *J Cell Biol* **66**: 521–530, 1975.
11. Tobey RA, Different drugs arrest cells at a number of distinct stages in G_2. *Nature* **254**: 245–247, 1975.
12. Rao PN, G_2 arrest induced by anticancer drugs. In *Effects of Drugs on the Cell Nucleus* (Eds. Busch H, Crooke ST and Daskal Y), pp. 475–490. Academic Press, New York 1979.
13. Crissman HA, Wilder ME and Tobey RA, Flow cytometric localization within the cell cycle and isolation of viable cells following exposure to cytotoxic agents. *Cancer Res* **48**: 5742–5746, 1988.
14. Lanks KW and Lehman JM, DNA synthesis by L929 cells following doxorubicin exposure. *Cancer Res* **50**: 4776–4778, 1990.
15. Bair KW, Andrews CW, Tuttle RL, Knick VC, Cory M and McKee DD, $ArCH_2NHC(CH_2OH)_2CH_3$ derivatives. Effect of ring size, shape and side chain position on murine antitumor activity. *J Med Chem* **34**: 1983–1990, 1991.
16. Bellamy WT, Dorr RT, Bair KW and Alberts DS, Cytotoxicity and mechanism of action of 3 arylmethylaminopropanediols (AMAPs). *Proc Am Assoc Cancer Res* **30**: 562, 1989.
17. Zucker RM, Elstein KH, Easterling RE and Massaro EJ, Flow cytometric discrimination of mitotic nuclei by right-angle light scatter. *Cytometry* **9**: 226–231, 1988.
18. Shapiro HM, *Practical Flow Cytometry*, 2nd Edn. Alan R. Liss, New York, 1988.
19. Zucker RM, Wu NC, Krishan A and Silverman M, Synchronization of murine erythroleukemic cells: Nuclear volume measurements for monitoring cell cycle traverse. *Exp Cell Res* **123**: 383–387, 1979.
20. Manca A, Bassani B, Russo A and Pacchierotti F, Origin of aneuploidy in relation to disturbances of cell-cycle progression. I. Effects of vinblastine on mouse bone marrow cells. *Mutat Res* **229**: 29–36, 1990.
21. Dean PN and Jett JH, Mathematical analysis of DNA distributions derived from flow microfluorometry. *J Cell Biol* **60**: 523–527, 1974.

22. Dolbeare F, Gratzner HG, Pallavicini MG and Gray JW, Flow cytometric measurement of total DNA content and incorporated bromodeoxyuridine. *Proc Natl Acad Sci USA* **80**: 5573–5577, 1983.
23. Latt SA and Langlois RG, Fluorescent probes of DNA microstructure and DNA synthesis. In: *Flow Cytometry and Sorting* (Eds. Melamed MR, Lindmo T and Mendelsohn ML), 2nd Edn, pp. 249–290. Wiley-Liss, New York, 1990.
24. Zucker RM, Elstein KH, Easterling RE and Massaro EJ, Flow cytometric analysis of the mechanism of methylmercury cytotoxicity. *Am J Pathol* **137**: 1187–1198, 1990.
25. Sorensen CM and Eastman A, Mechanism of *cis*-diamminedichloroplatinum (II)-induced cytotoxicity: Role of G_2 arrest and DNA double-strand breaks. *Cancer Res* **48**: 4484–4488, 1988.
26. Lock RB and Ross WE, Inhibition of $p34^{cdc2}$ kinase activity by etoposide or irradiation as a mechanism of G_2 arrest in Chinese hamster ovary cells. *Cancer Res* **50**: 3761–3766, 1990.
27. Traganos F, Darzynkiewicz Z and Melamed MR, The ratio of RNA to total nucleic acid content as a quantitative measure of unbalanced cell growth. *Cytometry* **2**: 212–218, 1982.
28. Crissman HA, Darzynkiewicz Z, Tobey RA and Steinkamp JA, Normal and perturbed Chinese hamster ovary cells: Correlation of DNA, RNA, and protein content by flow cytometry. *J Cell Biol* **101**: 141–147, 1985.
29. Hill AB and Schimke RT, Increased gene amplification in L5178Y mouse lymphoma cells with hydroxyurea-induced chromosomal aberrations. *Cancer Res* **45**: 5050–5057, 1985.
30. Darzynkiewicz Z, Probing nuclear chromatin by flow cytometry. In: *Flow Cytometry and Sorting* (Eds. Melamed MR, Lindmo T and Mendelsohn ML), 2nd Edn, pp. 315–340. Wiley-Liss, New York, 1990.
31. Evenson DP, Traganos F, Darzynkiewicz Z, Staiano-Coico L and Melamed MR, Effects of 9,10-anthracenedione, 1,4-bis[[2-[(2-hydroxyethyl)amino]-ethyl]amino]-, diacetate on cell morphology and nucleic acid of Friend leukemia cells. *J Natl Cancer Inst* **64**: 857–866, 1980.
32. Nakamura T, Masuda K, Matsumoto S, Oku T, Manda T, Mori J and Shimomura K, Effect of FK973, a new antitumor antibiotic, on the cell cycle of L1210 cells *in vitro*. *Jpn J Pharmacol* **49**: 317–324, 1989.
33. Roberts JR, Allison DC, Donehower RC and Rowinsky EK, Development of polyploidization in taxol-resistant human leukemia cells *in vitro*. *Cancer Res* **50**: 710–716, 1990.
34. Hoy CA, Rice GC, Kovacs M and Schimke RT, Over-replication of DNA in S phase Chinese hamster ovary cells after DNA synthesis inhibition. *J Biol Chem* **262**: 11927–11934, 1987.
35. Zucker RM and Elstein KH, A new action for topoisomerase inhibitors. *Chem Biol Interact* **79**: 31–40, 1991.
36. Chow K-C and Ross WE, Topoisomerase-specific drug sensitivity in relation to cell cycle progression. *Mol Cell Biol* **7**: 3119–3123, 1987.
37. Estey E, Adlakha RC, Hittelman WN and Zwelling LA, Cell cycle state-dependent variations in drug-induced topoisomerase II mediated DNA cleavage and cytotoxicity. *Biochemistry* **26**: 4338–4344, 1987.
38. Kalwinsky DK, Look AT, Ducore J and Fridland A, Effects of the epipodophyllotoxin VP-16-213 on cell cycle traverse, DNA synthesis, and DNA strand size in cultures of human leukemic lymphoblasts. *Cancer Res* **43**: 1592–1597, 1983.
39. Heck MMS, Hittleman WN and Earnshaw WC, *In vivo* phosphorylation of the 170-kDa form of eukaryotic DNA topoisomerase II. Cell cycle analysis. *J Biol Chem* **264**: 15161–15164, 1989.
40. Moreno S and Nurse P, Substrates for $p34^{cdc2}$: *In vivo* veritas? *Cell* **61**: 549–551, 1990.
41. Murray AW and Kirschner MW, Dominoes and clocks: The union of two views of the cell cycle. *Science* **246**: 614–621, 1989.
42. Willingham MC, Cornwell MM, Cardarelli CO, Gottesman MM and Pastan I, Single cell analysis of daunomycin uptake and efflux in multidrug-resistant and -sensitive KB cells: Effects of verapamil and other drugs. *Cancer Res* **46**: 5941–5946, 1986.
43. Ross WE and Smith MC, Repair of deoxyribonucleic acid lesions caused by adriamycin and ellipticine. *Biochem Pharmacol* **31**: 1931–1935, 1982.
44. Zwelling LA, Michaels S, Erickson LC, Ungerleider RS, Nichols M and Kohn KW, Protein-associated deoxyribonucleic acid strand breaks in L1210 cells treated with deoxyribonucleic acid intercalating agents 4′-(9-acridinylamino)methanesulfon-*m*-anisidide and adriamycin. *Biochemistry* **20**: 6553–6563, 1981.
45. Shackney SE, Smith CA, Miller BW, Burholt DR, Murtha K, Giles HR, Ketterer DM and Pollice AA, Model for the genetic evolution of human solid tumors. *Cancer Res* **49**: 3344–3354, 1989.